RSC Advances

ROYAL SOCIETY OF CHEMISTRY

www.rsc.org/advances

Abstract

A hybrid bulk electrode coated with sulfur spheres and graphene has been assembled via a two-step electrochemical deposition for the first time. Close-packed and layer-by-layer sulfur spheres were successfully deposited on the carbon fiber paper. The flexible bulk electrode is based on carbon fiber paper that is highly conductive and robust toward electrochemical cycling. When evaluated as a potential cathode for lithium sulfur (Li-S) batteries, such electrode exhibits fine lithium storage capabilities by virtue of their advantageous structural features.

Keyword: Hybrid Bulk Electrode; Electrochemical Deposition; Lithium Sulfur Batteries

Zhi-Zheng Yang, Hui-Yuan Wang, Xiao-Bin Zhong, Wen Qi, Bang-Yong Wang and Qi-Chuan Jiang

Assembling Sulfur Spheres on Carbon Fiber with Graphene Coated Hybrid Bulk Electrodes for Lithium Sulfur Batteries

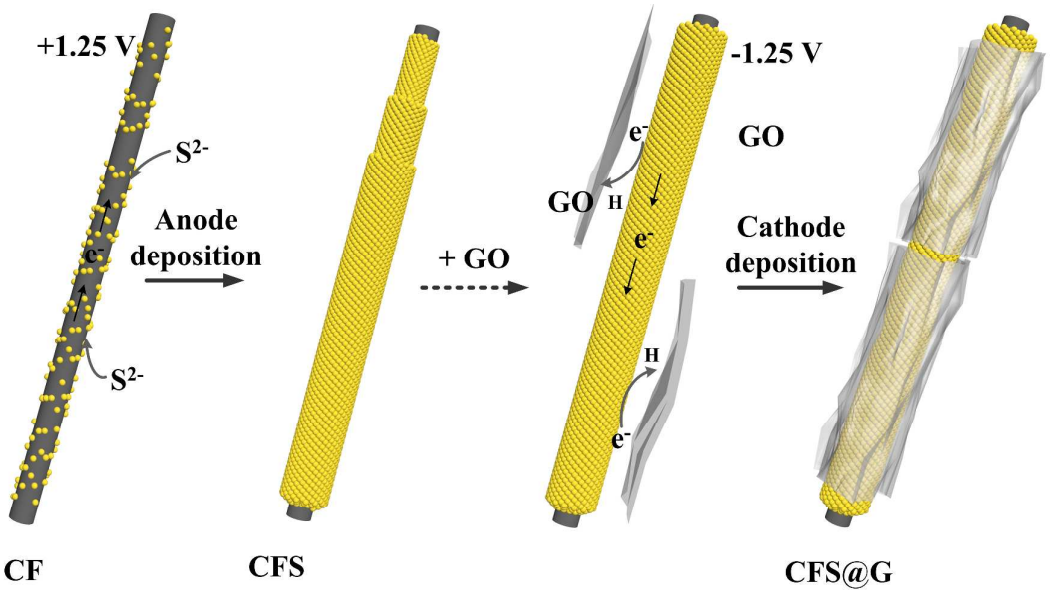

Journal Name

RSCPublishing

ARTICLE

Assembling Sulfur Spheres on Carbon Fiber with Graphene Coated Hybrid Bulk Electrodes for Lithium Sulfur Batteries

Cite this: DOI: 10.1039/x0xx00000x

Received 00th January 2012,
Accepted 00th January 2012

DOI: 10.1039/x0xx00000x

www.rsc.org/

Zhi-Zheng Yang, Hui-Yuan Wang,* Xiao-Bin Zhong, Wen Qi, Bang-Yong Wang and Qi-Chuan Jiang

A hybrid bulk electrode coated with sulfur spheres and graphene has been assembled via a two-step electrochemical deposition for the first time. Close-packed and layer-by-layer sulfur spheres were successfully deposited on the carbon fiber paper. The flexible bulk electrode is based on carbon fiber paper that is highly conductive and robust toward electrochemical cycling. When evaluated as a potential cathode for lithium sulfur (Li-S) batteries, such electrode exhibits fine lithium storage capabilities by virtue of their advantageous structural features.

Introduction

Because of the increasing energy and environmental issues, high energy density rechargeable batteries are in great demand for portable electronic devices.[1-3] Although lithium ion batteries (LIBs) have gained commercial success, they have not yet satisfied the needs for high-capacity applications such as power tools, electric vehicles or efficient use of renewable energies.[4-6] The challenge in post lithium ion research is to increase energy densities by utilizing high-capacity conversion cathodes such as sulfur or oxygen in combination with pure metal or metal oxide anodes.[7-9] Over the last 20 years, tremendous progress has been achieved in the design and fabrication of these anodes.[10-15] However, the existing cathode materials based on transition metal oxides or phosphates lead to significantly low energy densities, which have become a bottleneck for their wide commercialization, especially for high power applications.[2, 16] One of the most promising candidates for new energy storage options is the Li−S battery.[2, 3, 17] As a cathode, sulfur can host two lithium ions with the redox reaction of $S_8 + 16Li = 8Li_2S$, which provides five times higher theoretical energy density (2567 Wh kg $^{-1}$) than that of commercial LIBs.[3, 18] However, several challenges still exist for Li−S batteries, including the intrinsic low ionic/electronic conductivity of sulfur, dissolution of polysulfides in electrolytes, shuttling effect and large volume expansion during lithiation.[2, 8, 17] To solve these problems, much effort has been devoted to designing sulfur electrodes based on the composition and structure.[19-22]

Various carbon materials have been studied as conductive matrix to encapsulate sulfur and suppress the polysulfide shuttle effect.[21, 23, 24] Common carbon-based materials, such as carbon nanotubes, mesoporous carbon, hollow/porous carbon fiber and grapheme, have been used to improve sulfur cathode performance.[2, 3, 25] Despite the tremendous progress, there have been few promising approaches for mass production of sulfur cathodes. In addition, the fabrication of the carbon based S composites usually requires elaborate procedures, involving high-temperature and corrosive acid process for template synthesis.[23, 26] Such requirements significantly restrict the manufacturability of the S cathode materials. Therefore, the design and application of novel electrodes with high performance in a facile and flexible manner have demonstrated increasing significance.

Anodic deposition of sulfide ions is one of the important approaches to desulfurization of brines, tannery waste water and oil product.[27-29] In this work, we prepared a bulk electrode with sulfur packing on carbon fiber (CF) packed through a simple and economical anodic deposition approach. The sulfur spheres were grafted on carbon fiber (CFS) and then coated with graphene (CFS@G) via a novel cathode deposition. Compared with conventional methods, the fabrication of CFS@G electrodes can be scaled up easily for mass production. This unique structure is expected to manifest excellent lithium storage performance because of the integration of several advantageous structural features. Specifically, the highly conductive and flexible carbon fiber paper can provide a three-dimensional (3D) network to facilitate good transport of electrons. Besides, the sulfur spheres closely packed on the carbon fiber backbone are beneficial to the enhancement of electrochemical activity and the increase of internal void space. Furthermore, the outmost graphene coating around the electrode may serve as a structural buffering layer to alleviate the dissolution of polysulfides and the shuttling effect. Benefited from the enhanced kinetics for electron transport, our CFS@G hybrid electrodes exhibit a better capacity retention of 500-800 mA h g^{-1} at high current densities of 200-1000 mA g^{-1}.

Experimental

Preparation of CFS@G: Graphene oxide (GO) was prepared by the oxidation of natural graphite powder (Alfa, cat #43209, 325 mesh flakes) according to an improved method reported in the literature (see Supplementary Information for details).[30] The bulk CFS@G electrode was prepared by a two-step

electrochemical deposition at 25 °C. A two-electrode cell composed of the graphite as working electrode and a Pt mesh as counter electrode was assembled for the deposition process. After rinsed by ethanol and deionized water, carbon fiber paper (15 g m^{-2}, Jiangsu China) was pasted on a pure graphite flake electrode with Kapton tape along the side. The working-electrode compartment was injected with 0.2 M Na_2S solution as the electrolyte. Then the counter-electrode compartment (0.4 M NaOH filling solution) is separated from the working electrode by Nafion membrane that confines the product S_x to the anode compartment. After anode deposition at 1.25 V for 1 h using a CHI660D amperometry measurement under computer control, the electrode was immediately rinsed with deionized water and dried under 60 °C, denoted as CFS. The second deposition process was based on the same cell without Nafion membrane, and working-electrode replaced by bulk CFS. 0.5 mg mL^{-1} GO dispersion was served as the electrolyte. The cathode deposition of graphene was carried out under a constant potential of −1.25 V for 1 h. After deposition, the bulk electrode was washed with DI water to remove the residual GO absorbed on the electrodes. Finally, the bulk electrode was dried under 60 °C, denoted as CFS@G.

Structural Characterization: The crystalline phases were identified with X-ray diffraction (XRD, Dmax/2500PC, Rigaku, Japan) with Cu Kα radiation (λ=1.5406 Å). The morphology and structure of samples were characterized by a field emission scanning electron microscope (FESEM, JSM-6700F, Japan). Raman spectra were recorded with a Renishaw inVia Raman microscope (Britain) using an excitation wavelength of 633 nm. Thermogravimetric and differential thermal analysis (TG/DTA, SDT Q600, TA Instruments Inc. USA) were carried out to estimate the amount of sulfur in the CFS@G electrode under Ar flow (100 mL min^{-1}) at a heating rate of 10 °C min^{-1}.

Electrochemical Measurements： The prepared CFS@G electrode was dried at 60 °C for 12 h in a vacuum oven. The CR2025-type half-coin cells were assembled in an argon-filled glove box with H_2O and O_2 contents below 1 ppm. Metallic lithium foil was used as the counter and reference electrode. The electrolyte consisted of a solution of 1 M $LiCF_3SO_3$ in dimethoxyethane and dioxolane with a volume ratio of 50:50. Charge-discharge performances were evaluated by a LAND CT2001A battery instrument at a constant current density within a cutoff window of 1.5–3.0 V at room temperature. The total amount of graphene and sulfur active material in the working electrode was used to estimate the specific capacity of battery. Cyclic voltammogram measurements were carried out on an electrochemical workstation at a scan rate of 0.1 mV s^{-1} from 1.5 to 3.0 V. The electrochemical impedance spectroscopy analyses were performed with amplitude of 10 mV in the frequency range of 100 kHz to 100 mHz. Both cyclic voltammogram measurements and electrochemical impedance spectroscopy were carried out on the electrochemical workstation CHI650D (Shanghai Chen Hua Instruments Ltd.)

Discussion

The CFS@G bulk electrode was fabricated by a simple electrochemical deposition approach, as shown in Scheme 1 (for details, see Experimental Section). In the first step, carbon fiber was coated uniformly with close-packed and layer-by-layer sulfur spheres as shown by potentiostatic anode deposition. Electric field provided electrophoretic motion of anionic S^{2-} toward the anode and formed sulfur by electrolytic oxidation.[28] When applied, sulfur would build-up on the electrode surface. The sulfur deposition mechanism is probably due to the main reaction: $S^{2-} \rightarrow S+2e^-$.[28, 29] As a second step, graphene was wrapped around the CFS composites by potentiostatic cathode deposition. The deposition of GO was promoted by taking advantage of strong electrostatic attraction. The GO nanosheets deposited on the surface of CFS were reduced to graphene nanosheets by applying the negative potential. After the two-step electrochemical deposition, the bulk electrode CFS@G was formed.

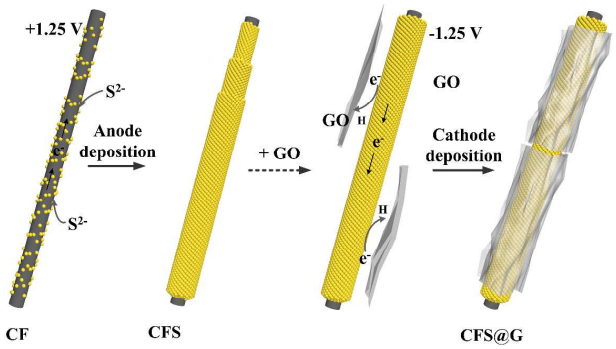

Scheme 1. Schematic illustration of the two-step electrochemical deposition for preparing the CFS@G bulk electrode.

The chemical compositions of the CF, CFS as well as CFS@G electrodes were determined by X-ray diffraction (XRD) analysis, with the results shown in Figure. 1. All of the samples exhibited a broad peak near 23°, which corresponded to the structure of the carbon fiber. For the pattern of CFS@G, vague diffraction peaks with low intensity located at around 24° can be assigned to graphene, which also suggested that the amount of graphene in the electrode was small. As compared with the XRD pattern of CF, new diffraction peaks were observed for the CFS and CFS@G bulk electrodes. The typical new peaks were indexed as the elemental sulfur (JCPDS card No. 08-0247). Therefore, the sulfur was successfully formed through the electrochemical deposition process.

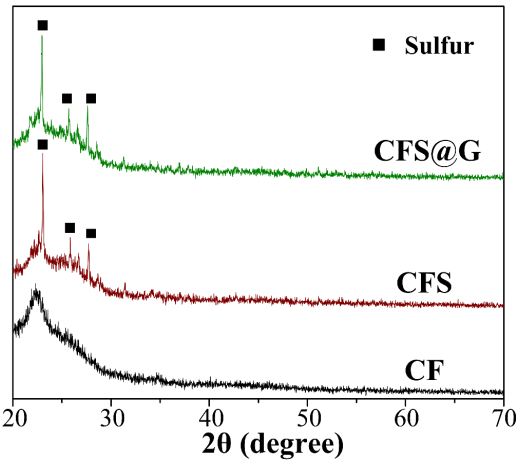

Figure 1. XRD patterns of the carbon fiber, sulfur loaded carbon fiber and sulfur loaded carbon fiber@graphene electrode.

The morphology and microstructure of the CF, CFS as well as CFS@G electrodes were examined by field-emission scanning

electron microscope (FESEM). The carbon fiber paper was prepared as the substrate for the uniform growth of sulfur spheres. The low-magnification FESEM image (Figure 2 a) reveals that the substrate was composed of smooth carbon fibers with diameters of 6–7 μm. After deposition of sulfur, the fibers (Figure 2b) became rougher and thicker, demonstrating that the sulfur was well loaded on the fibers. From the FESEM image in Figure 2c, it was confirmed that the close-packed sulfur micron spheres uniformly coated on the carbon fiber. In addition, the sulfur spheres that are also observed at a higher magnification (Figure 2d) form interconnected layer-by-layer film. In the case of CFS@G electrode in Figure 2e, the close-packed and layer-by-layer sulfur spheres were reserved after the graphene deposition. Figure 2e and 2f revealed several graphene nanosheets on the outer surface of the sulfur spheres, indicating coaxially coating of graphene on the CFS fiber. The graphene deposition was self-aligned, vertically oriented due to strong electrostatic attraction.[31-34] Raman spectroscopy in Figure S1 (Supporting Information) indicate the low graphitization of the CFS@G electrode. The peaks at 1345 and 1590 cm^{-1} correspond to D band and G band of graphene sheets, respectively.[35]

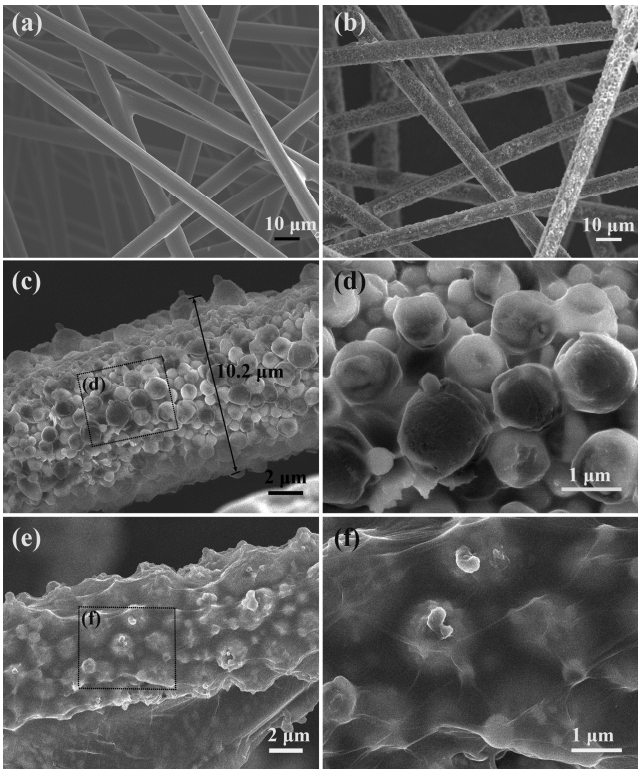

Figure 2. a) FESEM images of the carbon fiber paper; b, c, d) sulfur loaded carbon fiber and e, f) sulfur loaded carbon fiber@graphene electrode.

To test the electrochemical performance of the CFS@G bulk electrode, coin cells were assembled using a metallic Li foil as anode. The as-synthesized bulk electrode CFS@G was directly used as the cathode electrodes without any binder or conductive additives. The specific capacities were calculated based on the graphene and sulfur mass, according to the weight difference between carbon fiber paper and CFS@G. Unlike the conventional sulfur electrode preparation approach that involves Al foil current collector and carbon additive, the CFS@G electrode used in this work could highly reduce the total weight of the electrode. Although the sulfur mass was only 33wt % determined by TGA measurement in Figure S2 (Supporting Information), the typical areal density loading of active S was 0.8-1.3 mg/cm^2 based on the mass difference before and after the electrochemical deposition.

For further study of the electrochemical properties, charge/discharge voltage profiles were shown in Figure 4a at a current density of 200 mA g^{-1} between 1.5 V and 3.0 V (vs. Li^+/Li). The initial discharge capacity is 1017 mA h g^{-1}, which corresponds to 60% of the theoretical capacity of sulfur (1675 mA h g^{-1}). The first cycle possesses a lower voltage at the second plateau than the subsequent cycles, which may result from the interaction between sulfur and graphene in CFS@G electrode at the beginning of the discharge process. The two well defined plateaus become shorter upon cycling but persist throughout the first 50 cycles, which indicates a good stability. Compared with CFS@G, the CFS shows only a 27 % retention of the initial capacity (1075 mA h g^{-1}) after 50 cycles with the rapid fading of voltage plateau (Figure. 4b). The cycling performance of the CFS@G and CFS bulk electrodes at 200 mA g^{-1} are shown in Figure 4c. The reversible capacity of CFS@G still remains 500 mA h g^{-1} at 200 mA g^{-1} after 50 cycles, which is much higher than that of CFS. In addition, the coulombic efficiency of the CFS@G bulk electrode is more than 96 %, showing a better cycling stability than the electrode of CFS. Such a fine reversible capacity can certainly be attributed to the graphene shells, which provids protection against the shuttling effect and volume changes of sulfur spheres.[36, 37] However, this bulk electrode didn't maintain the capacity at a higher value after 50 cycles. We conjecture the reason is that there was not enough hollow space between the sulfur spheres for the volume expansion during the cycling process and the size of the sulfur spheres was not small enough.

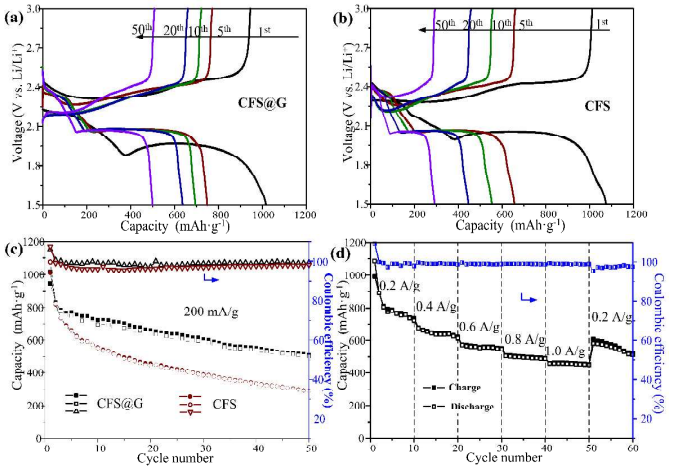

Figure 3. Galvanostatic discharge-charge test for (a) CFS@G; (b) CFS profiles at 200 mA g^{-1} for selected cycles; c) cycle performance of CFS@G; c) cycle performance of CFS@G at different specific currents.

The cycling behavior was evaluated at variable rates as shown in Figure.4d. As expected, CFS@G electrode manifests an exceptionally high rate capability. With the increase in rate, the capacity decreases constantly to 650 mA h g^{-1} for 0.4 A g^{-1}, 570 mA h g^{-1} for 0.6 A g^{-1}, 500 mA h g^{-1} for 0.8 A g^{-1}, 460 mA h g^{-1} for 1 A g^{-1} and increases to 600 mA h g^{-1} for 0.2 A g^{-1} after 50 cycles, respectively.

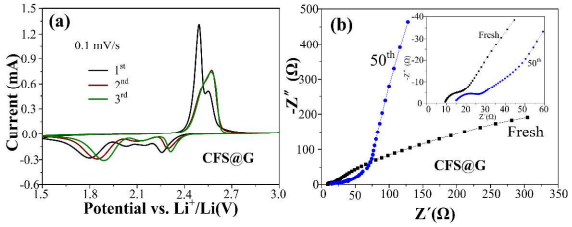

Figure 4. a) Cyclic voltammograms at scan rate of 0.1 mVs^{-1}; b) EIS spectra of the cell at different cycles for CFS@G.

Figure 4a depicted the typical cyclic voltammetry (CV) curves at a constant scan rate of 0.1 mV s^{-1} in the potential range of 1.5–3.0 V (vs. Li/Li^+) for the first three cycles. Two pronounced cathodic peaks at approximately 2.26 and 1.79 V are observed on the first cycle, which are consistent with what has been reported.[21, 22] The first peak at 2.26 V corresponds to the reduction of elemental sulfur to lithium polysulfide (Li_2S_n, 4<n<8). The peak at 1.79 V involves the further reduction of low order lithium polysulfide to Li_2S_2 and eventually to Li_2S. In the subsequent cathodic scan, the intensity of reduction peak current increases slightly. Two anodic peaks are observed in the potential around 2.49 V and 2.55 V, which is associated with the formation of Li_2S_n (n>2) in the charging stage. As cycling proceeds, the two anodic peaks overlap and form one broad peak at about 2.55 V, which may be due to high over-potential for conversion of Li_2S to lithium polysulfide.[38] These CV results indicate that these graphene nanosheets are helpful to alleviate the dissolution of polysulfides and the shuttling effect. The bulk electrode CFS@G was also characterized by electrochemical impedance spectroscopy (EIS). Figure 4b shows the Nyquist plots of the AC impedance, both consist of a depressed semicircle in high frequency region and an oblique line in medium frequency region. The intersection of the semicircle on the real axis provides an approximate indication of the charge transfer resistance (R_{ct}). After 50th cycles, the R_{ct} values increase from 20 Ω to 28 Ω. This may be due to the slow accumulation of Li_2S on the bulk cathode,[38] which is consistent with the slight decrease in the capacity with cycle processing. The diffusion processes can be clearly related to the dissolution of Li_2S and the formation of sulfur. After 50 cycles, the diffusion resistance was increased from the EIS at low frequencies. This may be due to the gradual formation of polysulfides and low electrically conductive solid during the Li–S discharge reaction.[39]

Conclusions

In summary, we successfully fabricated a bulk electrode coated with sulfur spheres and graphene via electrochemical deposition for the first time. Close-packed and layer-by-layer sulfur spheres were successfully deposited on the carbon fibers. After wrapping with graphene, the electrode CFS@G exhibited better lithium storage capability of 500 mA h g^{-1}. The scalable deposition process is promising for the sulfur electrode design.

Acknowledgements

The authors acknowledge financial support from Youth Science and Technology Innovation Fund in Jilin University (No. 450060497007 and 450060487471) and Project 985-Materials Science & Engineering of Jilin University.

Notes and references

Key Laboratory of Automobile Materials of Ministry of Education & School of Materials Science and Engineering Nanling Campus, Jilin University, No. 5988 Renmin Street, Changchun 130025, P R China

E-mail: wanghuiyuan@jlu.edu.cn;

Electronic Supplementary Information (ESI) available: [details of any supplementary information available should be included here]. See DOI: 10.1039/b000000x/

References

1. C. H. Xu, B. H. Xu, Y. Gu, Z. G. Xiong, J. Sun and X. S. Zhao, *Energy & Environmental Science*, 2013, **6**, 1388-1414.
2. Y. Yang, G. Zheng and Y. Cui, *Chemical Society reviews*, 2013, **42**, 3018-3032.
3. Y. X. Yin, S. Xin, Y. G. Guo and L. J. Wan, *Angew Chem Int Ed*, 2013, **52**, 13186-13200.
4. Z.-S. Wu, G. Zhou, L.-C. Yin, W. Ren, F. Li and H.-M. Cheng, *Nano Energy*, 2012, **1**, 107-131.
5. J. Zhu, L. Bai, Y. Sun, X. Zhang, Q. Li, B. Cao, W. Yan and Y. Xie, *Nanoscale*, 2013, **5**, 5241-5246.
6. J. Tarascon and M. Armand, *Nature*, 2001, **414**, 359-367.
7. R. Marom, S. F. Amalraj, N. Leifer, D. Jacob and D. Aurbach, *Journal of Materials Chemistry*, 2011, **21**, 9938-9954.
8. P. G. Bruce, S. A. Freunberger, L. J. Hardwick and J. M. Tarascon, *Nature materials*, 2011, **11**, 19-29.
9. C. B. Bucur, J. Muldoon, A. Lita, J. B. Schlenoff, R. A. Ghostine, S. Dietz and G. Allred, *Energy & Environmental Science*, 2013, **6**, 3286-3290.
10. T. Q. Wang, X. L. Wang, Y. Lu, Q. Q. Xiong, X. Y. Zhao, J. B. Cai, S. Huang, C. D. Gu and J. P. Tu, *Rsc Advances*, 2014, **4**, 322-330.
11. J. Liu, K. Song, P. A. van Aken, J. Maier and Y. Yu, *Nano letters*, 2014, **14**, 2597-2603.
12. H. Mi, Y. Li, P. Zhu, X. Chai, L. Sun, H. Zhuo, Q. Zhang, C. He and J. Liu, *Journal of Materials Chemistry A*, 2014, **2**, 11254–11260.
13. W. Xu, J. Wang, F. Ding, X. Chen, E. Nasybulin, Y. Zhang and J.-G. Zhang, *Energy & Environmental Science*, 2014, **7**, 513-537.
14. Z. Zhang, Y. Wang, W. Ren, Q. Tan, Y. Chen, H. Li, Z. Zhong and F. Su, *Angewandte Chemie*, 2014, **53**, 5165-5169.
15. J. G. Kim, S. H. Lee, Y. Kim and W. B. Kim, *ACS applied materials & interfaces*, 2013, **5**, 11321-11328.
16. J. Christensen, P. Albertus, R. S. Sanchez-Carrera, T. Lohmann, B. Kozinsky, R. Liedtke, J. Ahmed and A. Kojic, *Journal of The Electrochemical Society*, 2012, **159**, R1.
17. A. Manthiram, Y. Fu and Y. S. Su, *Acc Chem Res*, 2013, **46**, 1125-1134.
18. X. Tao, F. Chen, Y. Xia, H. Huang, Y. Gan, X. Chen and W. Zhang, *Chem Commun (Camb)*, 2013, **49**, 4513-4515.
19. Y.-C. Lu, Q. He and H. A. Gasteiger, *The Journal of Physical Chemistry C*, 2014, **118**, 5733-5741.
20. X. Li, A. Lushington, J. Liu, R. Li and X. Sun, *Chem Commun (Camb)*, 2014.
21. Z. Zhang, Z. Li, F. Hao, X. Wang, Q. Li, Y. Qi, R. Fan and L. Yin, *Advanced Functional Materials*, 2014, **24**, 2500-2509.
22. Z. Liang, G. Zheng, W. Li, Z. W. Seh, H. Yao, K. Yan, D. Kong and Y. Cui, *ACS nano*, 2014, **8**, 5249-5256.
23. S. Xin, Y.-X. Yin, L.-J. Wan and Y.-G. Guo, *Particle & Particle Systems Characterization*, 2013, **30**, 321-325.
24. C. Zhang, H. B. Wu, C. Yuan, Z. Guo and X. W. Lou, *Angewandte Chemie*, 2012, **51**, 9592-9595.
25. X.-B. Cheng, J.-Q. Huang, Q. Zhang, H.-J. Peng, M.-Q. Zhao and F. Wei, *Nano Energy*, 2014, **4**, 65-72.
26. W. Li, G. Zheng, Y. Yang, Z. W. Seh, N. Liu and Y. Cui, *Proceedings of the National Academy of Sciences*, 2013, **110**, 7148-7153.
27. P. Wapner, S. Lalvani and G. Awad, *Fuel processing technology*, 1988, **18**, 25-36.

28. A. Chen and B. Miller, *The Journal of Physical Chemistry B*, 2004, **108**, 2245-2251.
29. B. G. Ateya, F. M. AlKharafi, A. S. Alazab and A. M. Abdullah, *Journal of Applied Electrochemistry*, 2007, **37**, 395-404.
30. D. C. Marcano, D. V. Kosynkin, J. M. Berlin, A. Sinitskii, Z. Sun, A. Slesarev, L. B. Alemany, W. Lu and J. M. Tour, *ACS nano*, 2010, **4**, 4806-4814.
31. X. Huang, X. Qi, F. Boey and H. Zhang, *Chemical Society reviews*, 2012, **41**, 666-686.
32. S. Pei and H.-M. Cheng, *Carbon*, 2012, **50**, 3210-3228.
33. S. Bai and X. Shen, *RSC Advances*, 2012, **2**, 64-98.
34. K. Sheng, Y. Sun, C. Li, W. Yuan and G. Shi, *Scientific reports*, 2012, **2**, 247.
35. A. C. Ferrari, J. C. Meyer, V. Scardaci, C. Casiraghi, M. Lazzeri, F. Mauri, S. Piscanec, D. Jiang, K. S. Novoselov, S. Roth and A. K. Geim, *Phys. Rev. Lett.*, 2006, **97**, 4.
36. S. Lu, Y. Cheng, X. Wu and J. Liu, *Nano letters*, 2013, **13**, 2485-2489.
37. F.-f. Zhang, X.-b. Zhang, Y.-h. Dong and L.-m. Wang, *Journal of Materials Chemistry*, 2012, **22**, 11452-11454.
38. X. a. Chen, Z. Xiao, X. Ning, Z. Liu, Z. Yang, C. Zou, S. Wang, X. Chen, Y. Chen and S. Huang, *Advanced Energy Materials*, 2014, **4**.
39. N. A. Cañas, K. Hirose, B. Pascucci, N. Wagner, K. A. Friedrich and R. Hiesgen, *Electrochimica Acta*, 2013, **97**, 42-51.